Newtonian Jet Stability

ROLLIN PETER GRANT and STANLEY MIDDLEMAN

University of Rochester, Rochester, New York

Although Newtonian jet stability has been the object of numerous experimental and theoretical studies, the total problem of jet disintegration is by no means solved. Theories available in the literature are only applicable to low-speed laminar jets in stagnant air. In practice, the stability of a liquid jet may be influenced by the ambient medium, turbulence in the nozzle, and the extent of development of the velocity profile. None of these factors has received adequate study. This work presents the beginning of a systematic evaluation of the role played by these factors in the destabilization of a liquid jet. Correlations are presented for predicting the stability of both turbulent and high-speed laminar jets in stagnant air.

An understanding of the stability of liquid jets is of importance in the design of fiber spinnerettes, fuel combustion chambers, and liquid extraction columns. In practice, such applications usually involve relatively complex flow geometries and liquids exhibiting shear and/or time-dependent rheological properties. An understanding of such complicated systems can best be achieved by obtaining information under conditions more amenable to quantitative analysis. This work reports on the stability of liquid Newtonian jets ejected from circular capillary tubing into stagnant air.

Although Newtonian jet stability has been the object of numerous experimental and theoretical studies, it must be recognized that the total problem of jet disintegration is by no means solved. It is true that various details of the overall stability process have been worked out to a reasonable degree of completion. However, there are many missing links in the description of the series of events commencing in a liquid reservoir and terminating with the breakup of a free jet. For example, the influence of ambient pressure, turbulence in the nozzle, and the degree of velocity profile development have not been investigated adequately, either experimentally or theoretically. One of the objects of this study is an understanding of the various phenomena which play a role in stabilizing or destabilizing a jet.

In describing jet stability, one usually refers to the behavior of the coherent portion of the jet, or breakup length, as a function of the jet velocity. Experimentally established relationships between the breakup length (L) and the jet velocity (V) are of the form shown in Figure 1. Most investigators (*12, 21, 23, 25, 27*) report similar relationships up to point F; however, past this point there still remains some confusion over the true shape of the breakup curve (*7*).

The section ABC and the velocity V^o are related to the fact that at very low flow rates the liquid simply drips out of the tube and does not form a jet with a definable breakup length. In most systems the velocity V^o is much smaller than the lowest desirable operating velocity, and it is acceptable to extrapolate the line DC through the origin.

The linear portion of the curve (ACD) is reasonably well described by Weber's analysis (*28*) for the breakup of a laminar Newtonian jet under the influence of surface tension forces alone. Such a jet is predicted to be unstable only to symmetrical disturbances. Although Haenlein (*7*) verified this result experimentally, he also found

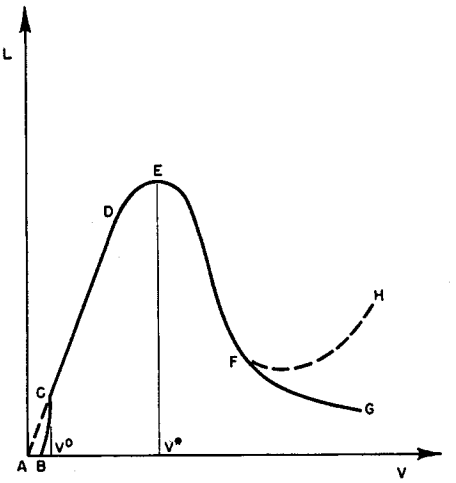

Fig. 1. General shape of breakup curve.

that the disintegration mechanism began to change from symmetrical drop breakup to transverse wave breakup somewhere between the velocities corresponding to points E and F.

Weber offered a possible explanation for this observation. He showed that aerodynamic forces acting on the surface of a jet tend to propagate both symmetric and transverse disturbances. Since aerodynamic forces become increasingly important as the jet velocity increases, the departure from linearity at point D and the subsequent behavior of the breakup curve could be ascribed to the influence of aerodynamic forces. While this is a plausible explanation, it is qualitative and has not been developed to the point where it permits one to predict the breakup curve. It is important to emphasize the lack of any theoretical or empirical correlation that accurately predicts either V^* or the L-V curve past point D.

It is apparent that there exists a great need for both well-defined experimental stability data and extensive theoretical exploration of many aspects of Newtonian jet stability. An objective of this work is to meet these needs by studying systems under such conditions that the data necessary to support a more complete understanding of Newtonian jet stability may be realized.

The specific areas to be investigated are, in review:

1. An independent experimental determination of the L-V curve under well-defined experimental conditions.
2. A subsequent attempt at predicting the breakup curve for an Newtonian liquid over a wide range of experimental conditions.

Rollin P. Grant is with Rohm and Haas Company, Bristol, Pennsylvania.

3. An experimental investigation of the roles of turbulence, ambient pressure, and velocity profile development in the stability process.

LITERATURE SURVEY

The problem of describing jet disintegration has been the object of theoretical and experimental investigation beginning as far back as 1833, with the work reported by Savart (*23*). Subsequent to Savart's experimental work, Plateau (*18*) and Rayleigh (*19*) contributed substantial quantitative descriptions of the stability mechanism. From potential energy considerations, Rayleigh was able to show that a cylinder of liquid in a vacuum and under the influence of surface tension forces alone is stable with respect to all classes of infinitesimal disturbances, except one. Specifically, the equilibrium configuration will always be unstable to a symmetrical disturbance whose wavelength exceeds the circumference of the undisturbed cylinder.

Assuming an inviscid liquid, Rayleigh obtained an equation for the growth rate of a given symmetrical disturbance. By assuming that the jet was destroyed by the disturbance possessing the maximum growth rate, Rayleigh finally obtained an expression for the wavelength and growth rate of the destructive disturbance. His theory was in complete agreement with Savart's experimental observations. The scope of this description was quite narrow, however, for it did not take into account either the viscosity of the liquid or the possible influence of the ambient medium upon the stability process.

The period following these analyses saw progress primarily from the addition of considerable experimental data to the literature (*7, 12, 21, 25, 27*).

Although subsequent to his analysis of the inviscid jet Rayleigh (*20*) incorporated viscosity into the problem, the complicated nature of his final equation made it of doubtful value. It was Weber, guided by the experimental work of Haenlein, who first obtained a quantitative description of the stability of a viscous jet. Weber considered the stability of a viscous jet under the influence of surface tension. By a tedious but straightforward process, Weber showed that the breakup length was a linear function of velocity for any given liquid and nozzle. For the viscous liquid, all other factors being equal, the predicted disintegration time exceeded that obtained from inviscid theory. Both of these results were in agreement with the experimentally observed behavior of the breakup length from *A* to *D*.

Although surface tension propagates only symmetrical disturbances, Weber succeeded in showing that aerodynamic forces tend to propagate both symmetric and transverse disturbances. Weber then reexamined the symmetrical breakup of a viscous jet. This time, however, he included aerodynamic effects. Results from this analysis predicted a maximum in the *L-V* curve, although the location of the maximum failed to agree with Haenlein's experimental data.

Castleman (*3*) and Lee and Spencer (*9*) followed with additional experimental contributions of a qualitative descriptive nature.

Tomotika (*26*) successfully introduced the viscosity of the ambient medium into the stability problem. However, the assumptions involved in his theory make it more directly applicable to the low-speed injection of one liquid into another.

Making use of dimensional analysis, Ohnesorge (*16*) developed a correlation which classified all jets into three distinct categories characterized by the destabilizing mechanism operative. This correlation was presented in the form of a logarithmic plot of the ratio $N_{We}^{1/2}/N_{Re}$, or the Ohnesorge number (*Z*), as it has since been designated, against N_{Re}. The three regimes were bounded by oblique straight lines of negative slope. At constant Ohnesorge number, the regions traversed with increasing Reynolds number were characterized by drop breakup, wave breakup, and atomization. The location of the boundary lines between these regimes was later modified by Littaye (*11*).

The more recent experimental studies of Fraser, Eisenklam, Dombrowski, and Hasson (*4*) and of Miesse (*15*) point out various features of the influence of ambient pressure on stability.

Thus, we have seen attempts at the description of the stability of liquid jets derived from theoretical considerations, dimensional analysis, and experimental observation. Although the theory has been developed to a high degree of sophistication, the simple fact remains that the best theory available, Weber's, does not accurately predict the breakup curve past point *D*. In general, the correlations that have been derived from dimensional analysis are inadequate, although they should give direction to future work. Despite all that has appeared in the literature on the subject of ambient pressure effects, it is a fact that no breakup length data are to be found. Although Weber developed a theory that takes into account ambient pressure effects, to our knowledge no one has ever explored its validity by comparison with experimental data. Also, particularly in the case of atomization, it is difficult to separate ambient effects from those of turbulence.

Schweitzer (*24*) argued that the growth of surface disturbances subsequent to discharge from the nozzle could not alone account for the high degree of atomization usually observed. He suggested that this mechanism might be reinforced by turbulence and vortex motion in the nozzle. On the other hand, Lee and Spencer reported that although turbulence "accelerates the disintegration of the fuel jet by ruffling its surface close to the orifice, . . . it has relatively little disintegrating force in itself."

Lee and Spencer raised an additional point that is worthy of discussion. In the case of data reported in the literature, it is particularly difficult to define a single value for the critical Reynolds number corresponding to the breakdown of laminar flow. When the length-to-diameter ratio of a nozzle becomes less than 5 or 10, it is quite likely that the concept of a single critical Reynolds number may be inapplicable. The geometry of the nozzle entrance and upstream flow conditions are bound to be important under such conditions. Also, since many investigators have been careful to isolate their equipment from disturbances, it is reasonable to assume that laminar flow might persist to relatively high values of the Reynolds number. Asset and Bales (*1*) claimed to have laminar flow up to a Reynolds number of 8,910. Hooper (*6*) reported an oscillation between laminar and turbulent flow at a Reynolds number of about 10,000.

Miesse (*14*) reported some turbulent breakup length data for jets of water and liquid nitrogen injected into air. However, in Miesse's own words, "The apparatus was designed to simulate injectors in current use and no attempt was made to guarantee fully developed shear flow. Hence, the data obtained will be a function of the orifice design."

Recently, Panasenkov (*17*) and Borisenko (*2*) further clouded the issue by reporting that the maximum in the breakup length curve for water jets injected into the atmosphere corresponded to a Reynolds number of 4,000 or 4,500. They claimed this to be the criterion for jet turbulence. This seems unlikely, since previous investigators have observed the maximization of the breakup curve at Reynolds numbers as low as 240 (*7*).

All indications to this point have been that turbulence either has no effect or tends to destabilize the jet. Once again, however, no well-defined breakup length data are to be found in the literature.

Rupe (*22*) observed that high velocity laminar jets may actually be more unstable and break up in an extremely violent fashion much sooner than fully developed turbulent jets. This is completely contrary to previous information in the literature. Rupe believed this behavior to be related to the decay of the fully developed laminar profile.

The earliest reference in the literature that may be related to the role of profile development is reported in the work of Smith and Moss (*25*). They noticed that their results differed rather markedly from Savart's in one respect, notably that Savart reported no maximum in the *L-V* curve. However, they noted that an important difference between their work and that of Savart was the manner in which the jets were produced. Smith and Moss believed that the different behavior of the jets could be ascribed to the difference in the emergent velocity profiles.

Hooper (*6*) described a bursting breakup as "a form of breakup hitherto unknown." In this case the jet consisted of a smooth glassy section followed by a region of complete and sudden atomization. He believed that the decay of the laminar parabolic profile to a flat profile supplied kinetic energy which

was converted into an internal pressure bursting the jet. To substantiate the theory, he reported the breakup length of the bursting jet to be independent of ambient pressures ranging from 1 to 0.031 atm.

Rupe commented that the decay of the parabolic velocity profile results in the creation of a radial pressure gradient which produces a radial velocity component. He believed that this radial velocity led to disintegration of the jet.

As in the previous cases, except for the work of Hooper, there exist no breakup length data in the literature to either support or refute the comments that have been made regarding the role of velocity profile development.

In addition to the more pertinent references cited, Miesse (*14*) and Krzywoblocki (*8*) have presented fine survey papers of much additional information peripheral to the general problem of characterizing jet stability.

REVIEW OF WEBER'S THEORY

In this section a brief review is presented of the major theoretical analysis of the stability of Newtonian jets. A good outline of the theory can be found in reference *10*; a critical and detailed review can be found in reference *5*.

As a starting point it is assumed that a surface disturbance may be written as a Fourier series involving terms of the form

$$\bar{\delta}(z, t) = \bar{\delta}_o e^{\alpha t + ikz} \tag{1}$$

in a coordinate system fixed to the jet, whose origin $z = 0$ was at the tube exit at $t = 0$. Weber (*28*) presented an analysis of jet stability which assumed the disturbances to be symmetric about the jet axis and sufficiently small so that inertial forces were unimportant. After considerable manipulation, a characteristic equation for α was found.

If the ambient fluid is assumed to exert neither radial nor shear stresses (jet in a vacuum or low-speed jet in a gas), the result is

$$\alpha^2 F_1 + \alpha F_2 \frac{3\mu\zeta^2}{\rho a^2} = \frac{\sigma}{2\rho a^3}(1 - \zeta^2)\,\zeta^2 \tag{2}$$

F_1 and F_2 are ratios of Bessel functions whose arguments include α and k. It can be shown that the curve of α vs. ζ goes through a maximum, and hence there is a disturbance at some wave number which grows most rapidly.

The jet is assumed to be subject to a spectrum of disturbances of the form of Equation (1), but to suffer disruption under the action of the disturbance with the largest growth rate α^*. If it is assumed that breakup occurs when the disturbance is comparable to the jet radius, then the breakup time T is given by

$$\bar{\delta}(o, t) = a = \bar{\delta}_o e^{\alpha^* T} \tag{3}$$

or

$$T = (1/\alpha^*)\ \ln\ (a/\bar{\delta}_o) \tag{4}$$

The breakup length is $L = VT$ or

$$L = (V/\alpha^*)\ \ln\ (a/\bar{\delta}_o) \tag{5}$$

For low-speed jets it is observed that $\zeta < 1$. It can be shown that the solution of Equation (2) can then be obtained with good approximation by setting $F_1 = F_2 = 1$. One easily finds α^* from the quadratic equation that results from Equation (2). Equation (5), in terms of dimensionless variables, becomes

$$L/D = [\ln\ (a/\bar{\delta}_o)]\ (N_{We}{}^{1/2} + 3\,N_{We}/N_{Re}) \tag{6}$$

The parameter $\ln(a/\bar{\delta}_o)$ must be determined experimentally. Weber reported a value of 12 based on the data of Haenlein.

In a further analysis, Weber included the pressure effects of an inviscid atmosphere. The characteristic equation for α becomes

$$\alpha^2 F_1 + \alpha F_2 \frac{3\mu\zeta^2}{\rho a^2} = \frac{\sigma}{2\rho a^3}(1 - \zeta^2)\,\zeta^2 + \frac{\rho_A V^2}{2\rho a^2}\zeta^3 F_3 \tag{7}$$

where F_3 is another ratio of Bessel functions with α and ζ in their arguments. When air effects are important no approximations for F_1, F_2, or F_3 are permissible, and Equation (7) must be solved numerically for α vs. ζ. The significant feature of Weber's analysis of the effect of the ambient medium is the prediction of a maximum in the L-V curve.

EXPERIMENTAL

A detailed discussion of the experimental features of this work is presented in reference *5*. The apparatus consisted of a high-pressure reservoir, a constant-temperature bath, a nozzle assembly, a Pyrex vacuum chamber, and high-speed photographic equipment. The jets were ejected horizontally.

In constructing the piping system through which liquid was transported from the reservoir to the nozzle entrance, particular attention was given to two details. First, the magnitude of the flow rate upstream of the nozzle entrance was held to a minimal value by choosing the largest feasible inside diameter for the components of the delivery system. Second, special care was taken to eliminate disturbances that are introduced by the sudden expansions and contractions that are normally encountered in flow through valves and fittings. In this apparatus all of the components of the delivery system, including the orifice of the ball valve in open position, had an I.D. of 0.375 in. In addition, the entire delivery system was securely anchored to a 35-lb. steel base plate. Thus every attempt was made to maintain an undisturbed and relatively quiescent flow field upstream of the nozzle entrance.

The entire experimental apparatus, exclusive of the vacuum pump and the nitrogen cylinders used to pressurize the reservoir, was mounted on a 3 ft. × 13 ft. table which in turn rested upon a vibration isolation pad.

All nozzles were constructed from stainless steel hypodermic tubing, square cut on both ends and burr free. Two separate techniques were used for mounting the nozzles but in all cases the tubes were mounted in a reentrant configuration, as illustrated in Figure 2.

The longer nozzles were supplied by the Becton Dickinson Company and attached to the delivery system by means of a conventional Luer-Lok fitting. The shorter nozzles, made in

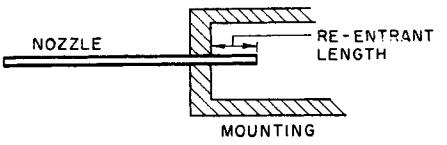

Fig. 2. Geometry of tube entrance.

TABLE 1. NOZZLE DIMENSIONS

Nozzle	Nozzle diameter, cm.	Length, cm.	l/D ratio	Mounting technique	Reentrant length,* cm.
1	0.137	14.0	102	Luer-Lok	0.7
2	0.138	1.02	7.4	Swagelok cap	0.3
3	0.137	0.98	7.2	Swagelok cap	0.3
4	0.0860	8.90	104	Luer-Lok	0.7
5	0.0840	4.29	51	Swagelok cap	0.5
6	0.0840	2.19	26	Swagelok cap	0.5
7	0.0865	0.60	6.9	Swagelow cap	0.1
8	0.0620	5.90	95	Luer-Lok	0.7
9	0.0310	4.90	148	Luer-Lok	0.7

* See Figure 2.

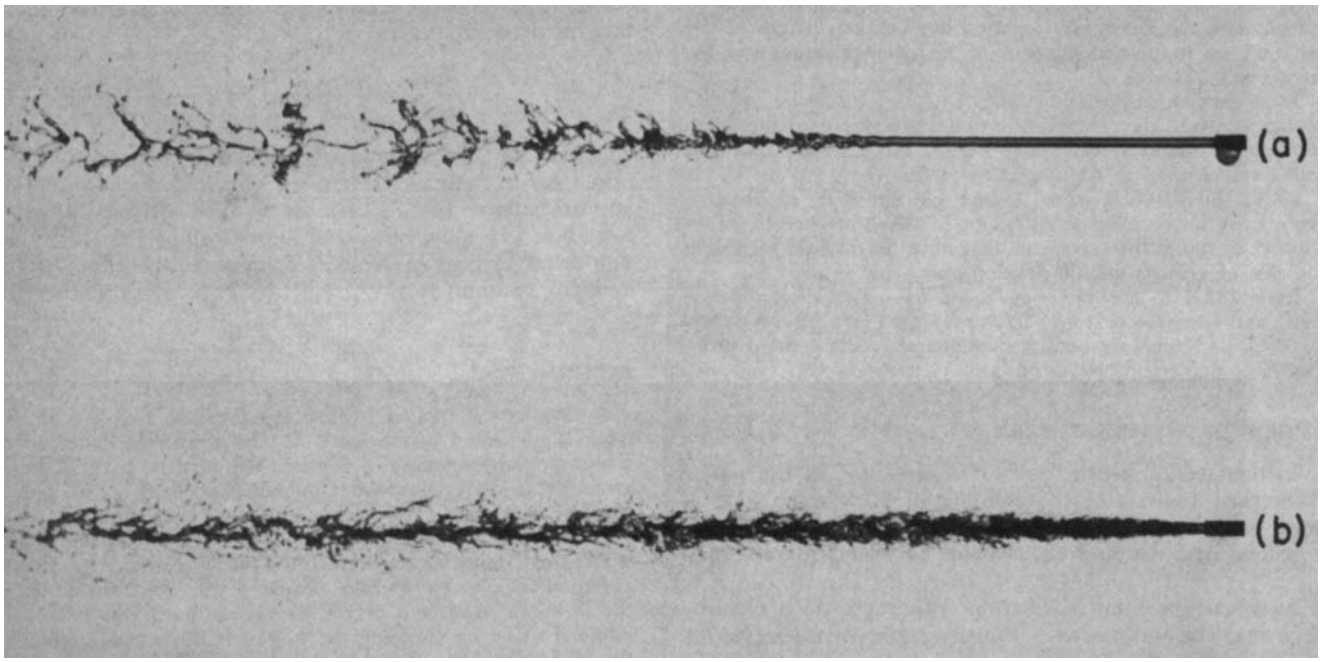

Fig. 3. *(a)* Laminar jet showing bursting breakup. *(b)* Turbulent jet.

the University of Rochester Engineering Shop, were mounted in half-inch Swagelok plugs.

All nozzles were examined under a 32× microscope and carefully deburred with a jeweler's broach, with particular care being taken to avoid beveling the corners. By using a traveling microscope accurate to 0.001 cm., measurements were made across several diameters to insure the absence of any deviation from a true circular opening. All pertinent data on nozzle dimensions are tabulated in Table 1.

Photographs were taken with a high-speed electronic flash unit and a 4 × 5 Graflex camera. The flash unit, a Model 549 Microflash manufactured by the Edgerton, Germeshausen & Grier Company of Boston, Massachusetts, delivered a 50 × 10^6 beam candle power flash of 0.5 μsec. duration.

All breakup data represent measurements made directly from negatives. Depending upon the order of magnitude of the dimensions involved, a traveling microscope accurate to 0.001 cm., a calibrated eyepiece accurate to 0.01 cm., or a simple scale accurate to 0.1 cm. was employed. Typical photographs are shown in Figure 3.

A tabulation of each of the experimental solutions used in these studies along with pertinent physical properties appears in Table 2. All physical properties reported were measured at 25.0°C. with standard techniques.

Table 2. Physical Properties of Working Solutions

Designation	Composition	Viscosity, poise	Density, g./cm.	Surface tension, dynes/cm.
1	Glycerine-water (approx. 88 wt. % glycerine)	1.62	1.235	62.8
2	Glycerine-water (approx. 72 wt. % glycerine)	0.26	1.190	64.5
3	Ethylene-glycol	0.179	1.116	48.2
4	Ethanol-water (approx. 95 wt. % ethanol)	0.0132	0.802	23.3
5	Distilled water	0.0091	0.997	71.0

All physical properties were measured at 25°C., which was the operating temperature for all systems reported herein.

Since solutions were run as many as a dozen times, it was necessary to guard against contamination and to monitor physical properties periodically. Solutions were frequently strained and surface tensions and viscosities checked. While no problems were encountered with surface tension variations, it was occasionally necessary to add small amounts of pure glycerine to the ethylene-glycol solution to combat its apparent hygroscopic tendency.

Upon blending a new solution for study, the initial step was the measurement of all physical properties. Subsequent to this the reservoir was loaded and constant-temperature conditions established. Once a nozzle had been selected, a velocity-reservoir pressure curve was obtained. This curve was generated by measuring the timed weight of effluent liquid at each of several pressures. All subsequent calculations were then based on the average velocity in the jet tube.

During the actual data taking, all pumps and stirrers associated with the thermostating system were shut off, eliminating all vibrations from the experimental equipment.

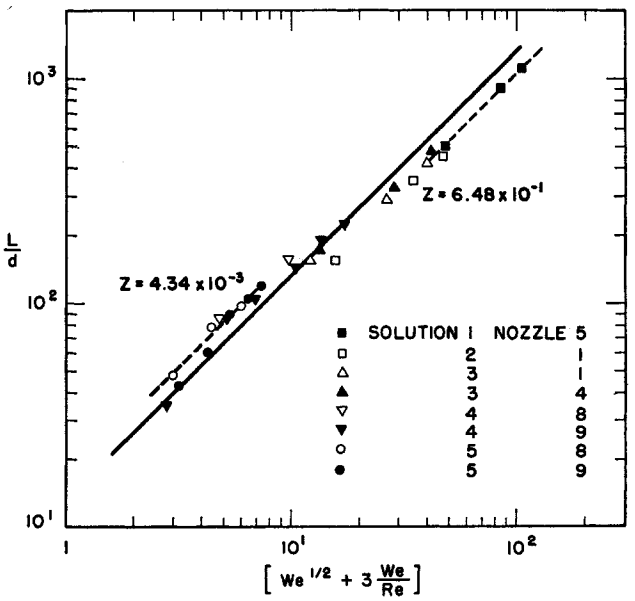

Fig. 4. Dimensionless correlation of low-speed breakup data. See Tables 1 and 2 for notation in key.

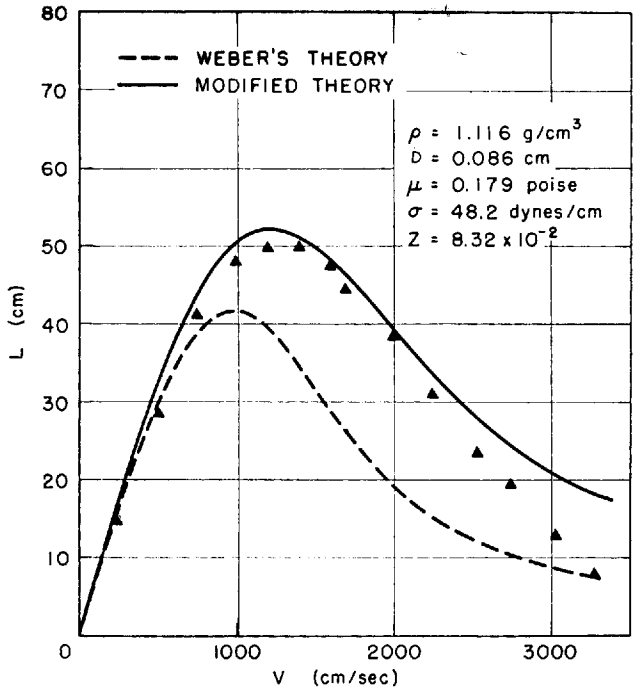

Fig. 5. Breakup curve for ethylene-glycol.

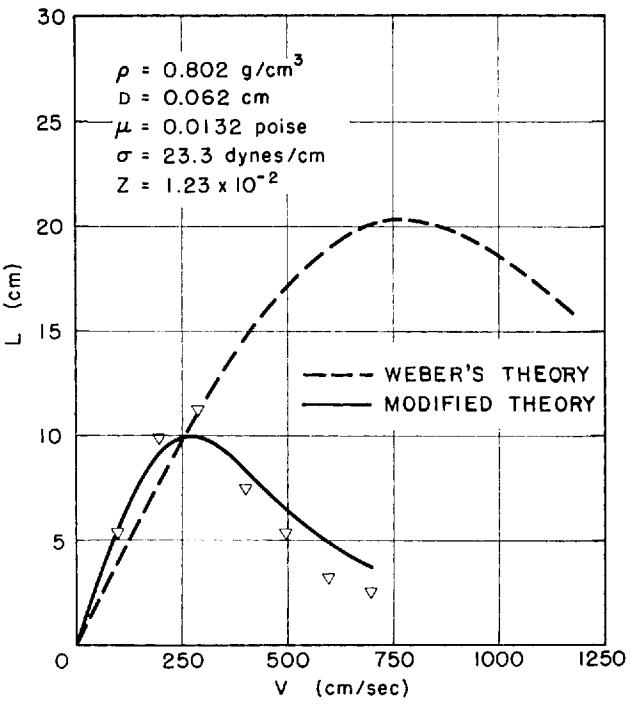

Fig. 6. Breakup curve for ethanol-water.

After dimming the lights and installing an appropriate pressure gauge on the reservoir, the jet was started. In most cases the jets were allowed to run for a minimum of 15 to 20 sec. before the first of a series of from four to eight photographs were taken. Thus, data points at each velocity represent the average of a minimum of four separate photographs.

CORRELATION OF DATA

Analysis of the data indicated that the average breakup lengths calculated from a series of photographs of the same event showed standard deviations which were generally less than 5% of the average, with occasional "bad" points showing standard deviations of 25%.

The Linear Portion (AD) of the Breakup Curve

Equation (6), which is derived directly from Weber's theory for the breakup of a laminar viscous jet in a vacuum, suggests a form of dimensionless correlation of the low speed linear portion of the breakup curve.

Figure 4 shows the linear breakup data plotted according to Equation (6). A line of unit slope, in agreement with Equation (6), gives an intercept of 13.4. This value for $\ln(a/\bar{o}_o)$ compares favorably with the values of 12 and 13 reported by Weber and by Smith and Moss, respectively.

In reality, however, it is statistically impossible to put a least squares line of unit slope through the data in Figure 4. The best straight line has a slope of 0.85 ± 0.02. Therefore, Equation (6) is not a valid general correlation for linear breakup data.

The reason for the failure of Equation (6) becomes apparent with the examination of two sets of linear breakup data corresponding to the extreme Ohnesorge numbers studied. In Figure 4 these data are fitted with separate lines of unit slope. Intercepts of 10.7 and 16.5 are obtained for Ohnesorge numbers of 6.48×10^{-1} and 4.34×10^{-3}, respectively. This shows that the ratio of the nozzle radius to the initial amplitude of the destructive disturbance is not a universal constant, and suggests that this ratio may be a function of the Ohnesorge number. This is an important point, since the literature implies that $\ln(a/\bar{\delta}_o)$ is a universal constant for all systems.

In spite of the failure of Equation (6), the least squares fit of the data in Figure 4 remains as a useful correlation for linear breakup data. The equation for the best line through the data in Figure 4 is

$$L/D = 19.5\,(N_{We}{}^{1/2} + 3\,N_{We}/N_{Re})^{0.85} \qquad (8)$$

Equation (8) correlates the data with a root-mean-square error of 12%. Since Equation (8) becomes invalid as the jet velocity approaches V^*, the use of this equation will require a companion correlation for V^*.

The Prediction of V^*

From a practical point of view, the final goal of any analysis of jet stability is the generation of a complete L-V curve for a given nozzle and liquid. Although the efforts of Weber represent a sound analysis of the breakup of a laminar jet, his theory is not entirely consistent with experimental observation.

Figures 5 and 6 compare breakup data with Weber's theory and indicate that the theory sometimes overestimates and sometimes underestimates the breakup curve.

The most interesting feature of Weber's analysis of symmetrical breakup with air effects is that it predicts a maximum in the L-V curve. This suggests that despite its failure to predict V^* correctly, the form of Equation (7) is essentially correct. The problem now becomes one of seeking a modification of this equation that will bring the predicted L-V curves into agreement with experiment. Modifications will be sought by examining the deviation of theory from experiment to determine if it occurs in a systematic fashion. Although such an approach is empirical in nature, this procedure will generate information of value in guiding future theoretical and experimental work.

Prior to the actual modification of Weber's theory, a correlation for V^* will be sought. The velocity V^*, in addition to being of practical importance, describes a unique point on the L-V curve. As such, it represents an extremely useful reference point.

From dimensional analysis one can argue that V^* should appear in a functional relationship of the form

$$N_{Re}{}^* = f(Z, \rho/\rho_A) \qquad (9)$$

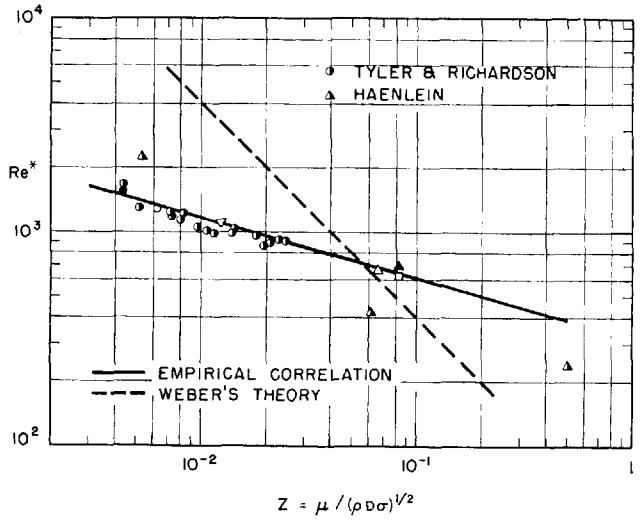

Fig. 7. Correlation of data on V^*.

where N_{Re}^* is based on V^*. Equation (9) suggests that a correlation of V^* might be obtained by plotting N_{Re}^* against Z for constant ρ/ρ_A. The Ohnesorge number represents a particularly attractive dimensionless group to correlate against, since it is independent of velocity and so is a constant for a given nozzle and liquid.

The V^* data were obtained over a 19-fold range in Z (8.32×10^{-2} to 4.34×10^{-3}), but only a 1.5-fold range in ρ (1.19 to 0.802 g./cc.). Thus, since the ambient pressure was held constant, ρ/ρ_A was essentially constant with respect to Z for this particular set of data.

In Figure 7 experimental N_{Re}^* data are plotted as a function of Z. A statistically significant correlation is obtained with

$$N_{Re}^* = 325\,Z^{-0.28} \qquad (10)$$

In Figure 7, both this empirical correlation and Weber's theory are compared with additional data from the literature. Two points are significant. It is clear that Weber's theory does not predict the position of the observed maximum, as already implied. Of even more significance is the fact that the data of other workers seem to be consistent with ours. This is strong evidence that our results are not subject to the spurious effects that can be easily introduced into experimental studies of hydrodynamic stability.

The Modification of Weber's Theory to Predict the Entire Breakup Curve for a Laminar Jet

With the aid of Equation (10), it is now possible to attempt a modification of the theory. The modification will be conducted in two steps. The significance of each step is most easily appreciated by reexamining Equation (5). First, Equation (7) will be modified to force the ratio α^*/V to minimize at values of N_{Re}^* consistent with Equation (10). Second, predicted values of L^* will be forced to agree with experiment by treating $\ln(a/\delta_o)^*$ as a variable.

Equation (7) is modified by replacing F_3 with F_4, where F_4 is defined as a function of the Ohnesorge number and not ζ. The examination of the deviation between Weber's theory and data at the maximum leads to a definition of F_4 as

$$F_4 = 0.018\,Z^{-1.32} \qquad (11)$$

Equation (7), with F_3 replaced by F_4, is found to minimize the ratio α^*/V at values of N_{Re}^* in good agreement with those predicted by Equation (10).

The initial step in obtaining a correlation for $\ln(a/\bar{\delta}_o)^*$ is the multiplication of experimental L^* values by the corresponding ratios $(\alpha^*/V)^*$ calculated from Equation (7), with F_3 replaced by F_4. These values of $\ln(a/\delta_o)^*$ are plotted against the Ohnesorge number in Figure 8. The best (least squares) line through the data is represented by the equation

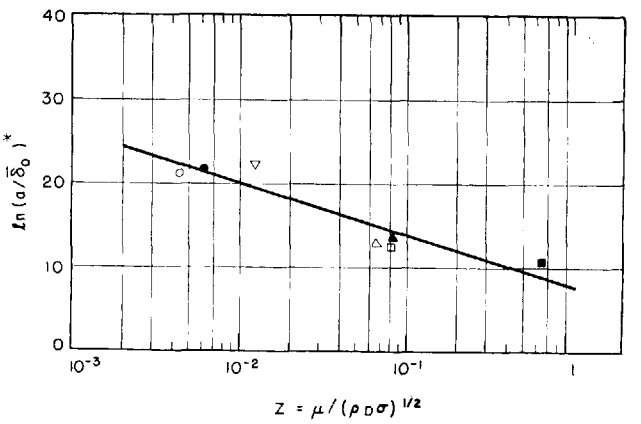

Fig. 8. Variation of $\ln(a/\bar{\delta}_o)^*$ with Ohnesorge number.

$$\ln(a/\bar{\delta}_o)^* = -2.66 \ln Z + 7.68 \qquad (12)$$

With the combination of Equations (5), (7) (with F_3 replaced by F_4), and (12) it is possible to predict the entire breakup curve. The complete calculation is carried out by a computer program, with only the Ohnesorge number required as input. Results from the modified theory are shown in Figures 5 and 6. The agreement with experiment is seen to be markedly improved in the region of V^* and beyond.

The treatment of $\ln(a/\bar{\delta}_o)$ as a variable requires some further comment. Equation (12) states that the larger the Ohnesorge number, the larger must be the initial amplitude of the destructive disturbance relative to the nozzle radius. This is consistent with the observation that the jet is more stable at large Ohnesorge numbers (that is, high viscosity and low surface tension) and therefore might require a larger initial disturbance to bring about instability.

The reader is reminded that the velocity (V) used in all correlations is the average velocity in the nozzle. Another velocity that might have been used is the velocity of

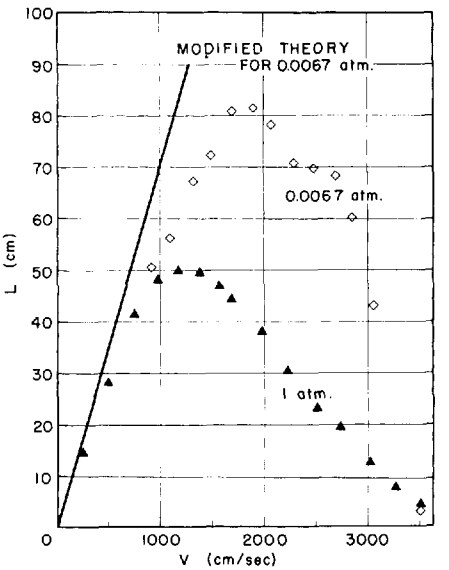

Fig. 9. Failure of modified theory to correlate data at subatmospheric pressure.

the jet surface. This velocity will differ from V for two reasons:

1. Since the jet undergoes a slight diameter change upon emerging from the nozzle, the average flight velocity will differ from V. The average flight velocity may be either larger or smaller than V, depending upon whether the jet contracts or expands (*13*).

2. Immediately upon emerging from the nozzle, the velocity of the jet surface will be zero. As the velocity profile relaxes, the surface velocity will approach the average flight velocity.

Since the surface velocity is obviously less easily defined than the average velocity in the nozzle, this explains the preferred use of the latter velocity in all correlations.

The Successes and Deficiencies of the Modified Theory

When combined and solved, Equations (5), (7), and (12) are found to predict breakup curves in good agreement with experiment. A logical test of the generality of the modified theory is to investigate the accuracy with which it predicts a breakup curve measured at subatmospheric pressure. In Figure 9, the atmospheric and subatmospheric data obtained with the solution 3-nozzle 4 system are compared with the modified theory. It is apparent that the modified theory still fails to account properly for the ambient medium, except at atmospheric pressure, where it was forced to do so.

All of the results reported thus far are for jets produced from nozzles of sufficient length to assure a fully developed velocity profile at the nozzle exit. The data shown in Figure 10 were obtained with tubes of varying length at constant diameter. It is apparent that for the linear portion of the data no l/D dependence is found. This is true even for the shortest tube, the length of which is insufficient to insure fully developed flow over the entire range of data shown. Apparently the velocity profile of the jet has no effect on the propagation of a disturbance growing in the linear range of instability.

However, beyond the linear portion of the curve, the short tube produces jets which are markedly more stable than those produced from longer tubes. This implies a coupling between the velocity profile in the jet and the mechanism of instability under conditions where air resistance becomes dominant in destroying the jet.

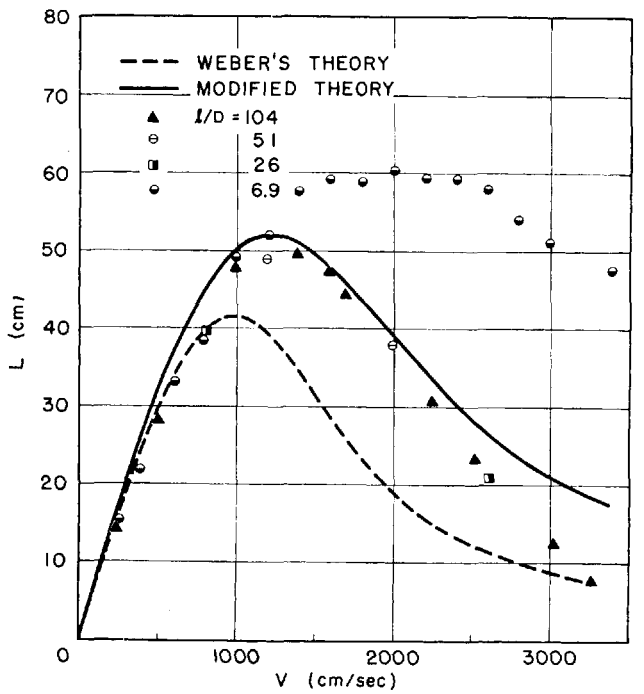

Fig. 10. Dependence of breakup length on l/D.

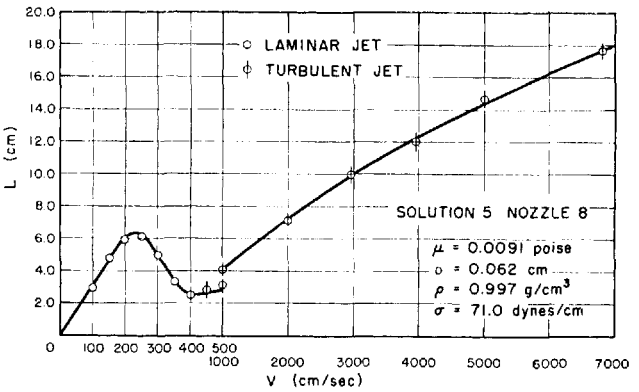

Fig. 11. Effect of transition to turbulence on breakup curve.

A possible explanation of this lies in the relaxation of the velocity profile of a jet ejected under fully developed conditions. The relaxing profile develops an inflection point at the jet surface, and inflection points in velocity are well known to be associated with flow instabilities.

It is difficult to draw a firm conclusion on this point because of a second characteristic of the shortest tube. Photographic evidence supported by the reservoir pressure-velocity calibration curve indicated that the jet detached itself from the tube wall at a velocity in the neighborhood of 1,800 cm./sec. The detached jet is in contact only with the tube entrance and so has a flat velocity profile. However, the jet is subject to a different environment as it travels detached through the tube than an attached jet with a nearly flat profile. Hence it is not clear that the profile *alone* is the source of enhanced stability over the entire range of data. However, the jet is attached between 1,000 and 1,600 cm./sec., and is more stable, in this region, than other jets differing *only* in the state of profile development. Our conclusion, somewhat weakened by the complication of a detached flow, is that a flat velocity profile enhances the stability of a jet under such conditions that air resistance is the principal destructive force.

Since a detached jet is in contact with only the nozzle entrance, it may be assumed to possess a flat velocity profile. Weber's theory assumes the jet to have a flat velocity profile. However, from Figure 10 it is obvious that neither Weber's theory nor the modified theory predicts accurately the breakup curve for a jet with a flat velocity profile beyond the linear portion of the curve.

The Turbulent Jet

Figure 11 shows a typical breakup curve covering both laminar and turbulent flow. It is interesting to note that turbulence apparently stabilizes the jet. This is a misleading conclusion, however, since stability mechanisms must be compared in terms of breakup time L/V, rather than breakup length. Calculations from Figure 11 indicate a decreasing breakup time with increasing velocity. This corresponds to an increase in the rate of growth of a disturbance with increasing velocity, that is, the jet becomes less stable as velocity is increased.

Figure 12 shows the turbulent breakup data plotted in dimensionless form. The square root of the Weber number is used as the independent variable because it is proportional to velocity. A least square line through the data is given by

$$L/D = 8.51\ (N_{We}{}^{1/2})^{0.64} \qquad (13)$$

Equation (13) correlates the data with a root-mean-square error of 9.4%. Although data are plotted for $N_{We}{}^{1/2} > 200$, experimental evidence indicates that the concept of a breakup length begins to lose its meaning at such large Weber numbers. Equation (13) may be used

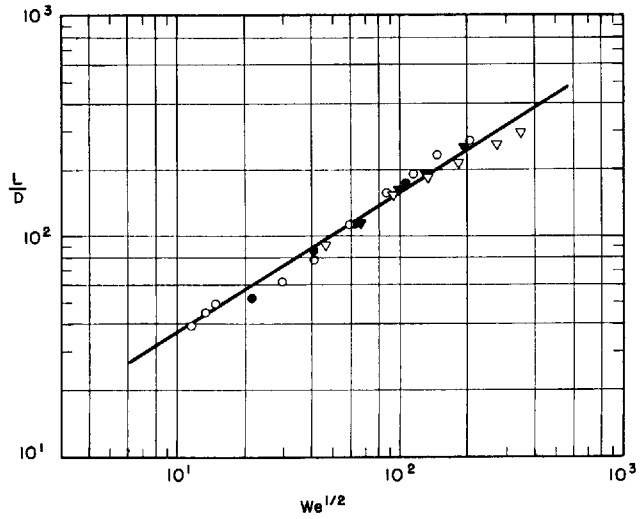

Fig. 12. Correlation of turbulent breakup data.

in conjunction with the modified theory for the laminar jet to complete the prediction of a complete breakup curve. Of course, it would be necessary to know the transition Reynolds number in the system of interest.

DETAILED OBSERVATIONS OF JET INSTABILITY

While the correlations presented here are of obvious engineering utility, they provide no insight into the various modes of instability operative under different conditions. Such information can be obtained only upon examination of photographs which show clearly the type of disturbance which ultimately destroys a given jet. In this section we show a few sequences of photographs obtained at atmospheric pressure, accompanied by comments on the character of the breakup observed. Detailed photographic sequences are presented in reference 5.

Solution 5-Nozzle 8 (Water)

Figure 13 shows a sequence of photographs from which a breakup curve of the shape *ADEFH* is obtained.

*Figure 13*a. (V = *148 cm./sec.*, N_{We} = *19.1*, N_{Re} = *1,008*). At a velocity of 148 cm./sec., the jet is seen to undergo a regular symmetric breakup. The small arrow shown on the photograph indicates the breakup point. In this instance, the choice of a breakup length is very straightforward.

*Figure 13*b. (V = *250 cm./sec.*, N_{We} = *54.5*, N_{Re} = *1,703*). The breakup pictured in this photograph is typical of the region immediately past V^*. A low amplitude transverse disturbance is observed about a third of the distance from the nozzle exit to the breakup point. It is barely visible in the reproduction shown here. The appearance of this wave is quite predictable, and it is present at approximately the same distance from the nozzle in all photographs of this fluid at this velocity. Downstream, the jet is once again destroyed by a symmetrical disturbance.

In this photograph the tendency of the jet to segment is observed, and the choice of the breakup length does not necessarily coincide with the first point at which the jet is broken. This comment requires some further discussion of the criteria employed in the selection of a breakup length.

The selection of the breakup length for a low-speed jet presents no particular problem, as demonstrated in Figure 13*a*. However, in the region of V^* and beyond, the choice of a meaningful and consistent value for the breakup length becomes increasingly difficult.

Only after examining hundreds of photographs of high-speed jets were criteria established for the choice of the breakup length. Criteria were sought which defined a reproducible value for the breakup length, and which defined a breakup length that could be quantitatively described. For example, it would be unreasonable to attempt the characterization of a breakup length defined by the first break in the jet. This length behaves very erratically over the *EF* portion of the breakup curve.

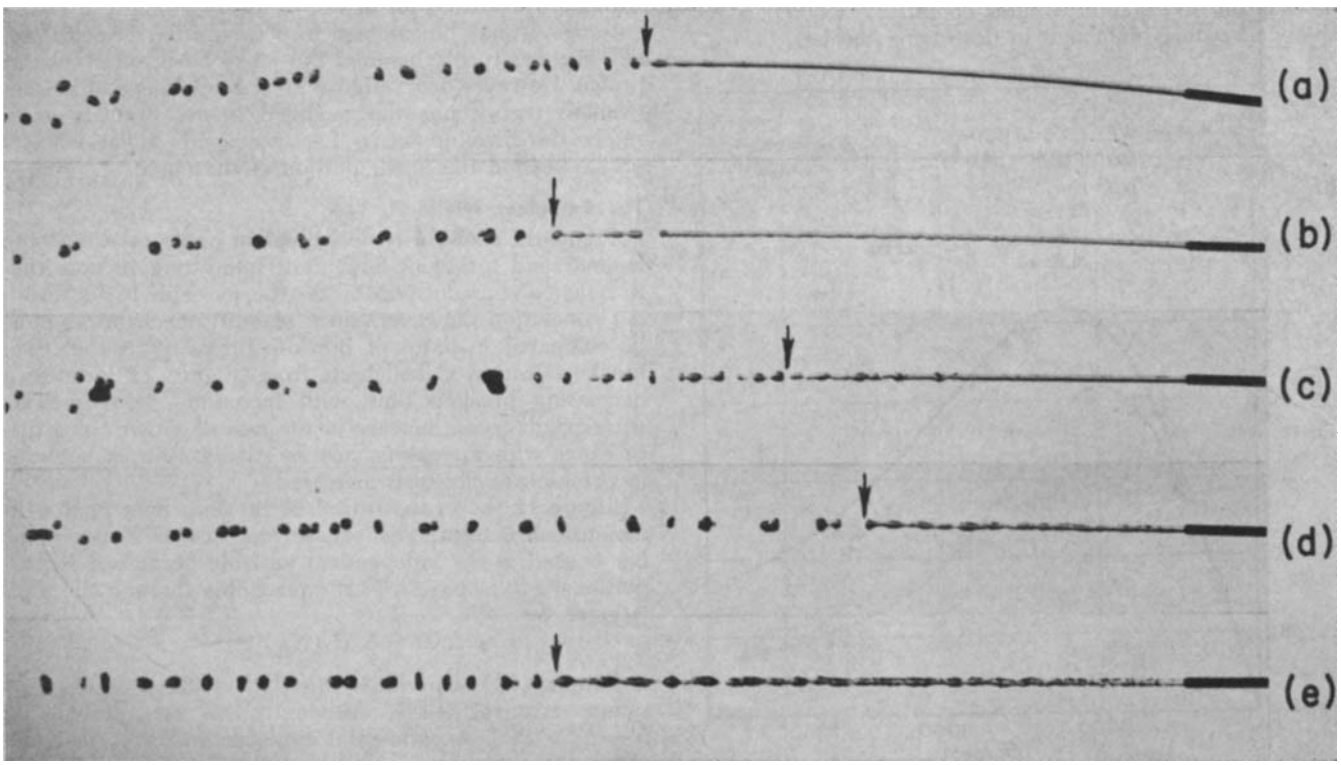

Fig. 13. Photographic sequence for water jet in air.

If the jet is ultimately destroyed by a symmetrical disturbance, the breakup point is taken as the place at which the most regular disturbance breaks the jet. A regular disturbance may be defined as one possessing a relatively constant wavelength. This criterion continues to apply when transverse waves appear on the jet, so long as they do not actually break the jet. The concept of wave breakup, as discussed in the literature, implies the actual destruction of the jet by a transverse disturbance.

*Figure 13*c. (V = *350 cm./sec.*, N_{We} = *107*, N_{Re} = *2,384*). The breakup pictured in this figure corresponds to the transition area between wave and drop breakup. Although rather severe waves are apparent, the jet is finally destroyed by a symmetrical disturbance. An interesting feature of photographs as this velocity is the continued appearance of the low amplitude wave at approximately the same distance from the nozzle exit. The breakup length has migrated closer to the point of appearance of this disturbance.

*Figure 13*d. (V = *400 cm./sec.*, N_{We} = *139*, N_{Re} = *2,725*). At this velocity the jet is seen to be ruffled at the nozzle exit. Although the jet is turbulent, it is still possible to define a breakup length. The high degree of atomization observed in other turbulent jets is absent in this case, since the transition velocity is so low.

Close examination of Figure 13 reveals the absence of the low amplitude transverse wave which appears in the two preceding figures. It is difficult to determine if the wave has actually disappeared or if it is simply masked by the ruffled character of the surface. In spite of the ruffled surface, however, the jet undergoes a symmetrical breakup.

*Figure 13*e. (V = *1,000 cm./sec.*, N_{We} = *875*, N_{Re} = *6,813*). The breakup length begins to increase once again, and the jet persists in being destroyed by a symmetrical disturbance.

Conclusions Based on Photographic Evidence

For curves of the shape *ADEFG*, Haenlein found V^* to represent the point at which the disintegration shifted from symmetrical to transverse wave breakup. However, photographs of our jets give only limited support to the findings of Haenlein.

If transverse wave breakup is taken to be the actual destruction of the jet by a transverse disturbance (as it is by Haenlein), then V^* is *not* found to correspond to a shift from symmetrical to transverse wave breakup. The presence of a maximum in the L-V curve is associated with the *appearance* of transverse waves on the jet, but the actual destruction of the jet by a transverse disturbance always occurs at a velocity greater than V^*. As the velocity of the jet is further increased, the low amplitude waves are no longer damped but grow very rapidly and destroy the jet.

The characterization of the breakup curves obtained at atmospheric pressure may be summarized as follows. Over the linear portion of all L-V curves, the jets are destroyed by a regular symmetrical disturbance. In the region of the velocity V^* the breakup remains symmetrical, but the tendency of the jet to segment is observed. All systems are characterized by the appearance of low amplitude transverse waves at velocities slightly in excess of V^*. Initially, these waves appear to damp, and the jet continues to be destroyed by a symmetrical disturbance. To this point, all systems behave in the same manner. As the velocity is further increased, two paths may be followed, depending upon whether the flow in the nozzle remains laminar or becomes turbulent.

If the flow in the nozzle becomes turbulent, the low amplitude waves either disappear or are masked by the ruffled character of the surface. Whatever the case, the turbulent jet initially is destroyed by a symmetrical disturbance. As the velocity of the turbulent jet is further increased, the symmetrical breakup gives way to transverse wave breakup. At very high velocities, surface atomization becomes severe, and the concept of a breakup length (as a measure of jet stability) begins to lose its meaning.

If the flow in the nozzle remains laminar, the low amplitude waves continue to appear. As the velocity is increased, transverse waves destroy the jet, and the breakup length decreases until it nearly coincides with the point at which the low amplitude waves first appear on the jet. When this occurs the jet is destroyed by a violent bursting disintegration mechanism. Once the bursting mechanism appears, it persists until the onset of turbulence in the nozzle.

ACKNOWLEDGMENT

The authors are grateful to the National Science Foundation for support of this research under Grant G 20563. We are indebted to Lever Brothers Company for fellowship support of Rollin P. Grant.

NOTATION

a = radius of jet, cm.
D = diameter of tube, cm.
F_1, F_2, F_3 = functions in characteristic equation for α
k = wave number of a disturbance, cm.$^{-1}$
L = breakup length, cm.
l = length of tube, cm.
N_{Re} = Reynolds number = $DV\rho/\mu$
N_{We} = Weber number = $V^2\rho D/\sigma$
t = time, sec.
T = LV = breakup time, sec.
V = average velocity in tube, cm./sec.
z = axial variable, cm.
Z = $(N_{We})^{1/2}/N_{Re}$ = Ohnesorge number = $\mu/(\rho D\sigma)^{1/2}$

Greek Letters

α = growth rate of a disturbance, sec.$^{-1}$
δ = amplitude of a disturbance, cm.
δ_o = initial amplitude of a disturbance, cm.
ζ = $2\pi a/\lambda = ka$
λ = wavelength of a disturbance, cm.
μ = viscosity of jet, poise
ρ = density of jet, g./cc.
ρ_A = density of ambient medium, g./cc.
σ = surface tension, dynes/cm.

Superscript

* = values defined at maximum in breakup curve

LITERATURE CITED

1. Asset, G. M., and P. D. Bales, *U. S. Army Chem. Corps Med. Lab. Res. Rept. No. 64* (1951).
2. Borisenko, A. I., *J. Tech. Phys. U.S.S.R.*, **23**, 195 (1953).
3. Castleman, R. A., *U. S. Natl. Bur. Standards J. Res.*, **6**, 369 (1931).
4. Fraser, R. P., Paul Eisenklam, Norman Dombrowski, and David Hasson, *A.I.Ch.E. J.*, **8**, 672 (1962).
5. Grant, R. P., Ph.D. thesis, Univ. Rochester, N. Y. (1965).
6. Hooper, P. C., Ph.D. thesis, London Univ. (1959).
7. Haenlein, A., *Natl. Advisory Comm. Aeronaut. Tech. Memo No. 659* (1932).
8. Krzywoblocki, M. Z., *Jet Propulsion*, **26**, 760 (1956).
9. Lee, D. W., and R. C. Spencer, *Natl. Advisory Comm. Aeronaut. Tech. Rept. No. 454* (1933).
10. Levich, V., "Physicochemical Hydrodynamics," Prentice-Hall, Englewood Cliffs, N. J. (1962).
11. Littaye, G., *Compt. Rend.*, **217**, 99 (1943).
12. Merrington, A. C., and E. G. Richardson, *Proc. Phys. Soc. London*, **59**, 1 (1947).

13. Middleman, Stanley, and J. Gavis, *Phys. Fluids*, **4**, 355 (1961).
14. Miesse, C. C., *Ind. Eng. Chem.*, **47**, 1690 (1955).
15. ———, *Jet Propulsion*, **25**, 525 (1955).
16. Ohnesorge, W., *Z. Angew. Math. Mech.*, **16**, 355 (1936).
17. Panasenkov, N. S., *J. Tech. Phys. U.S.S.R.*, **21**, 160 (1951).
18. Plateau, "Statique experimentale et theorique des liquides soumis aux seules forces molecularies," Rayleigh, Vol. II, pp. 360, 363, 364, Dover, New York (1945).
19. Lord Rayleigh, *Proc. London Math. Soc.*, **10**, 7 (1878); Lord Rayleigh, "Theory of Sound," Vol. II, pp. 351-365, Dover, New York (1945).
20. ———, *Phil. Mag.*, **34**, 153 (1892).
21. Richardson, E. G., *Appl. Sci. Res.*, **A-4**, 374 (1951).
22. Rupe, J. H., *Natl. Aeronaut. Space Admin. Tech. Rept. No. 32-207* (1962).
23. Savart, F., *Ann. Chim.*, **53**, 337 (1883); Lord Rayleigh, "Theory of Sound," Vol. II, pp. 362-364, Dover, New York (1945).
24. Schweitzer, P. H., *Penn. State Coll. Eng. Exp. Sta. Bull. No. 40*, Appendix I, 63-68 (1932).
25. Smith, S. W. J., and H. Moss, *Proc. Roy. Soc. London*, **A93**, 373 (1916-1917).
26. Tomotika, S., *Proc. Roy. Soc. London*, **A150**, 322 (1935).
27. Tyler, E., and B. A. Richardson, *Proc. Phys. Soc. London*, **37**, 297 (1925).
28. Weber, C., *Z. Angew. Math. Mech.*, **11**, 136 (1931).

Manuscript received July 23, 1965; revision received January 4, 1966; paper accepted January 14, 1966. Paper presented at A.I.Ch.E. Boston meeting.

Phase Equilibria in Polymer Solutions

J. F. HEIL and J. M. PRAUSNITZ

University of California, Berkeley, California

A new semiempirical equation is presented for the Gibbs energy of mixing for solutions of polymers in single and mixed solvents. The equation contains two adjustable parameters per binary mixture and can readily be extended to multicomponent systems without additional parameters. The new expression gives a very good representation of the properties of a variety of polymer solutions including those in which there are strong specific interactions such as hydrogen bonding. Parameters are determined from binary vapor pressure data.

A graphical method based on the new equation is given for predicting solubility limits in ternary systems containing one polymer and a mixed solvent. Only binary data are used. The method is demonstrated by comparisons of predicted solubility behavior with new experimental data taken on systems composed of polystyrene and the following mixed solvents: acetone-toluene, acetone-benzene, methanol-benzene, methanol-ethyl acetate, and acetone-methylcyclohexane.

The thermodynamics of polymer solutions has been discussed in many books (*10, 15, 17, 19, 25, 26, 29, 31*) and an excellent review of work prior to 1956 has been given by Tompa (*31*). Most previous work has been concerned with nonpolar solutions. In this work we present a new equation for the Gibbs energy of mixing for polymer solutions which appears to be useful for a large variety of systems including polar and hydrogen-bonded components.

The most widely known theoretical treatment of polymer solutions is that of Flory and Huggins. Flory (*11, 12*) and Huggins (*20, 21*) derived an expression for the entropy of mixing for athermal solutions containing monomeric solvent molecules and long-chain polymer solute molecules which consist of a number of contiguous segments, each equal in size to a solvent molecule. Their treatment applies only at concentrations such that the randomly coiled polymer molecules overlap one another extensively. A somewhat different treatment has been proposed for very dilute solutions (*13, 14*).

Extension of the theoretical athermal equation to nonathermal solutions was achieved semiempirically by the adoption of a van Laar term (*17, 27, 32*) for representation of the heat of mixing. The well-known expression for the molar Gibbs energy of mixing, known as the Flory-Huggins equation, is

$$\frac{\Delta g^M}{RT} = x_1 \ln \phi_1 + x_2 \ln \phi_2 + \chi \phi_1 \phi_2 (x_1 + m x_2) \quad (1)$$

From criteria of thermodynamic stability, it can be shown that at the critical point for incipient phase separation

$$\chi = \frac{1}{2}\left(1 + \frac{1}{\sqrt{m}}\right)^2 \quad (2)$$

Since m is usually very large, the Flory-Huggins theory predicts complete miscibility of polymer and solvent if

$$\chi \leq 1/2 \quad (3)$$

The Flory-Huggins equation does not generally provide a quantitative description of the thermodynamic properties of polymer solutions, because contrary to the theory, numerical values of χ, as deduced from experimental data, are often a strong function of polymer concentration even for nonpolar solutions. For example, as shown in Figure 1, the value of χ for solutions of cellulose derivatives in acetone changes markedly as the volume fraction of polymer is varied; similar changes in χ have been observed for many other polymer solutions.

Burrell (*6*) and Blanks (*5*) have proposed methods for the prediction of limited miscibility in polymer solutions based upon the Flory-Huggins equation and an extended form of the regular solution theory of Hildebrand (*17*). It appears that these methods cannot be extended to systems in which specific molecular interactions occur.

J. F. Heil is with Stauffer Chemical Company, Richmond, California.